Electronic Supplementary Material (ESI) for Physical Chemistry Chemical Physics.


# Supplementary Information

# How Do the Hydrocarbon Chain Length and Hydroxyl Group Position Influence the Solute Dynamics in Alcohol-Based Deep Eutectic Solvents?

**Sk Saddam Hossain and Anunay Samanta***

*School of Chemistry, University of Hyderabad, Hyderabad-500 046, India*

*E-mail of corresponding author: anunay@uohyd.ac.in*

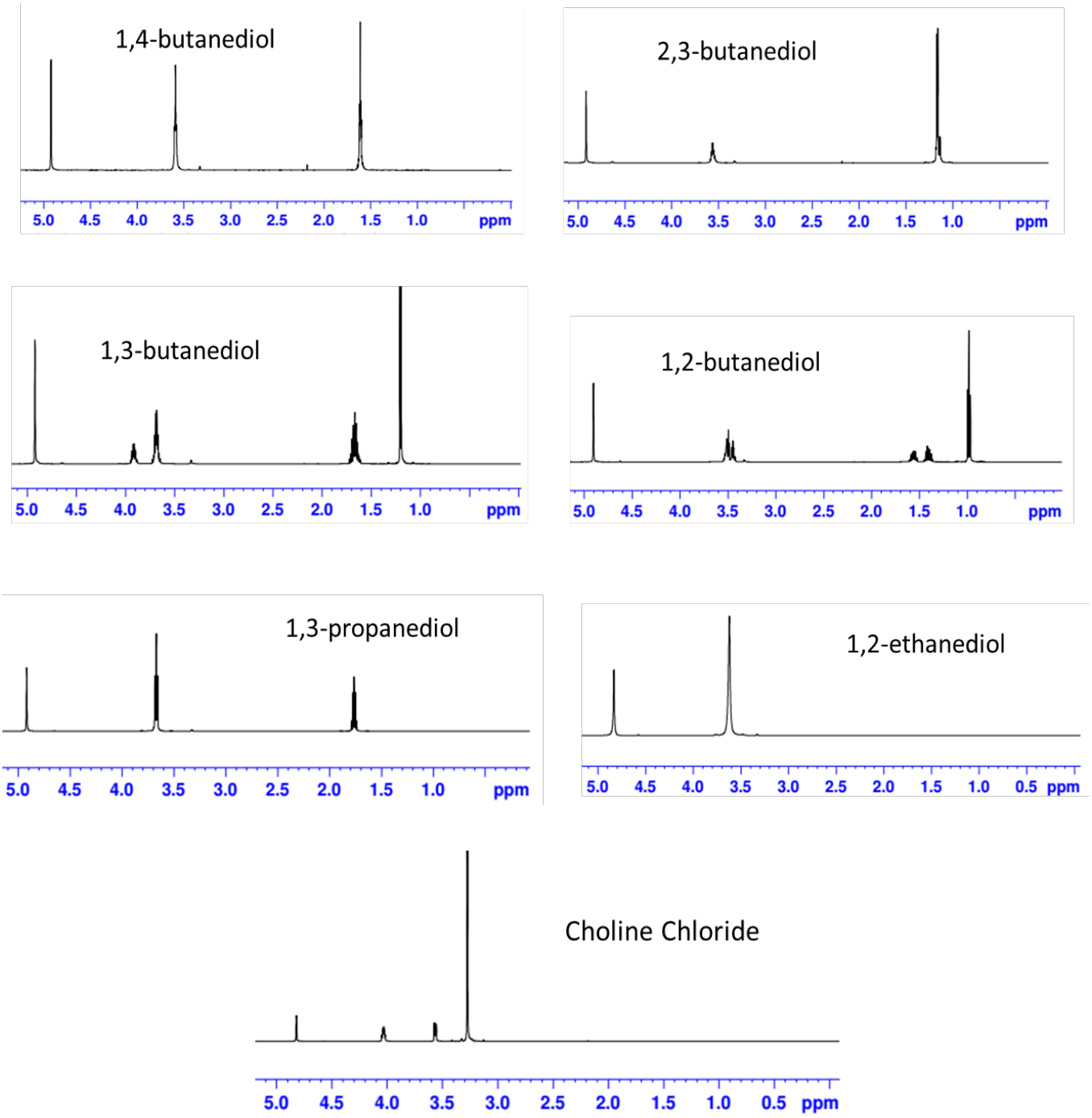


**Figure S1. $^{1}$H NMR spectra of different reagents (in $CD_3OD$) used for synthesis of DESs.**

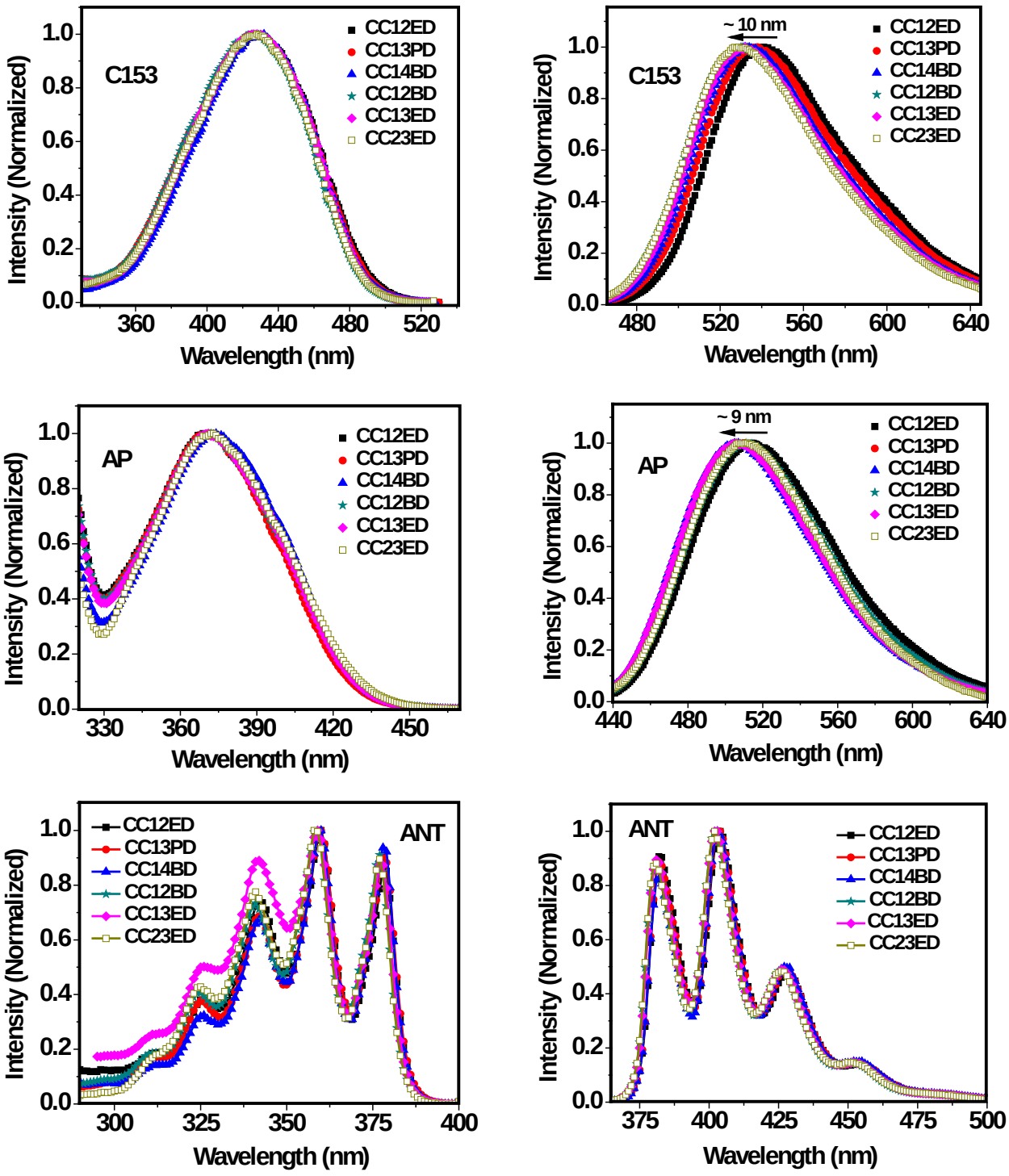


**Figure S2. Normalized excitation (left panel) and emission (right panel) spectra of the solutes in six DESs at 298K. The emission/excitation spectra are recorded by exciting the samples at their respective maxima of excitation/emission spectra.**

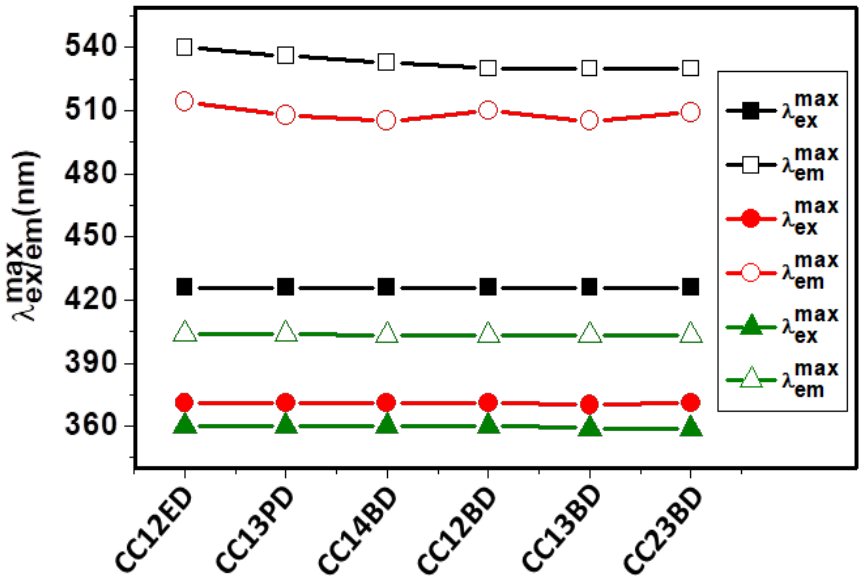


**Figure S3. Comparison of the changes of $\lambda_{ex}^{max}$ and $\lambda_{em}^{max}$ of C153 (square), AP (circle) and ANT(triangle) in six DESs at 298K.**

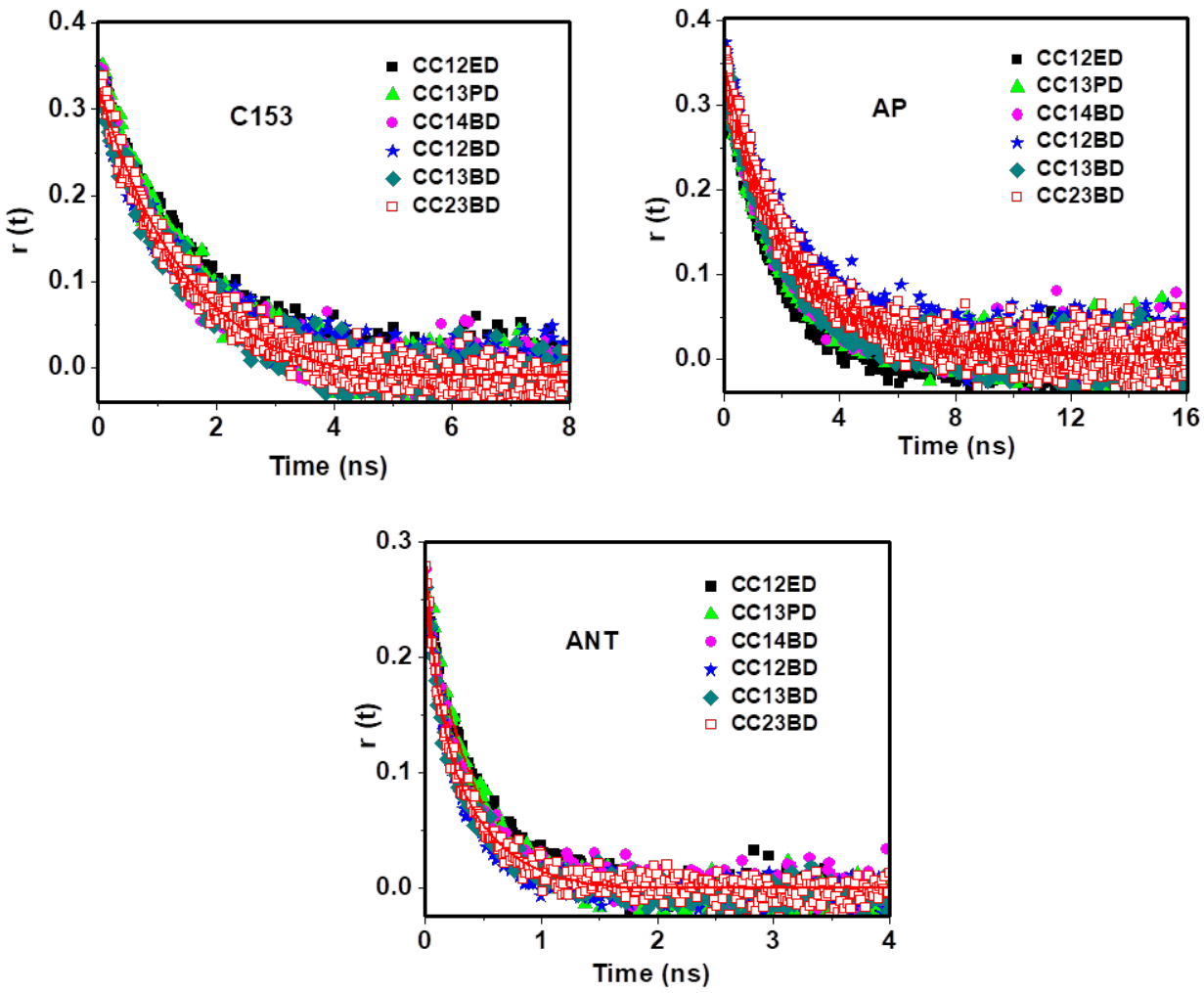


**Figure S4. Anisotropy decay profiles of the solutes in six DESs at isoviscous (30 cP) condition. The solid lines represent single-exponential fit to the decay profiles. The excitation wavelength for C153/AP and ANT are 405 and 375 nm, respectively. All the decay profiles are recorded by monitoring at respective emission maxima of solutes in six DESs.**

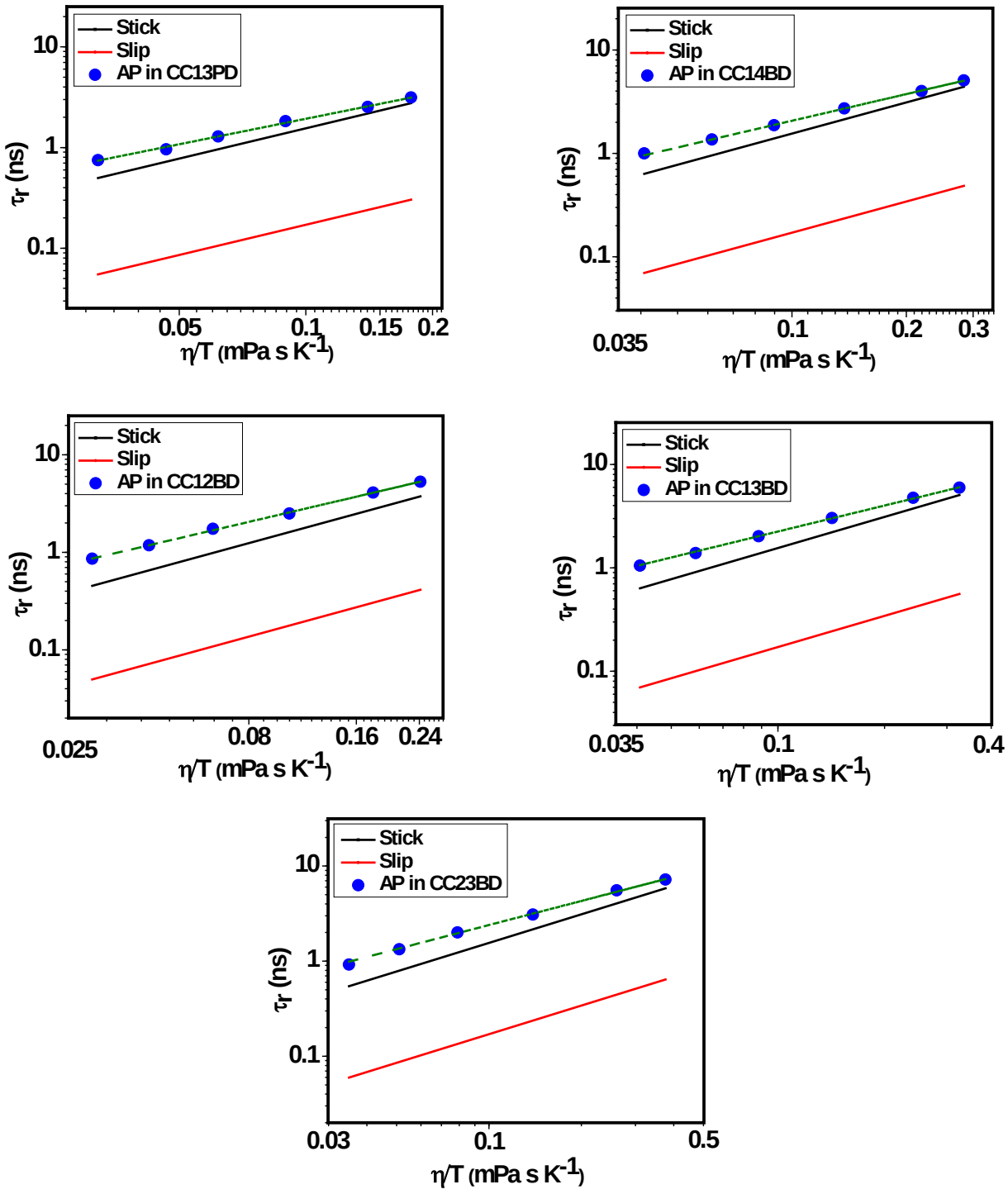


**Figure S5. Plots of $\tau_r$ vs η/T for AP in DESs. The solid circles indicate the experimental rotational times and the dashed lines represent fit to the data according to $\tau_r = A(\eta/T)^p$. Computed stick (black) and slip (red) lines using SED theory are also shown.**

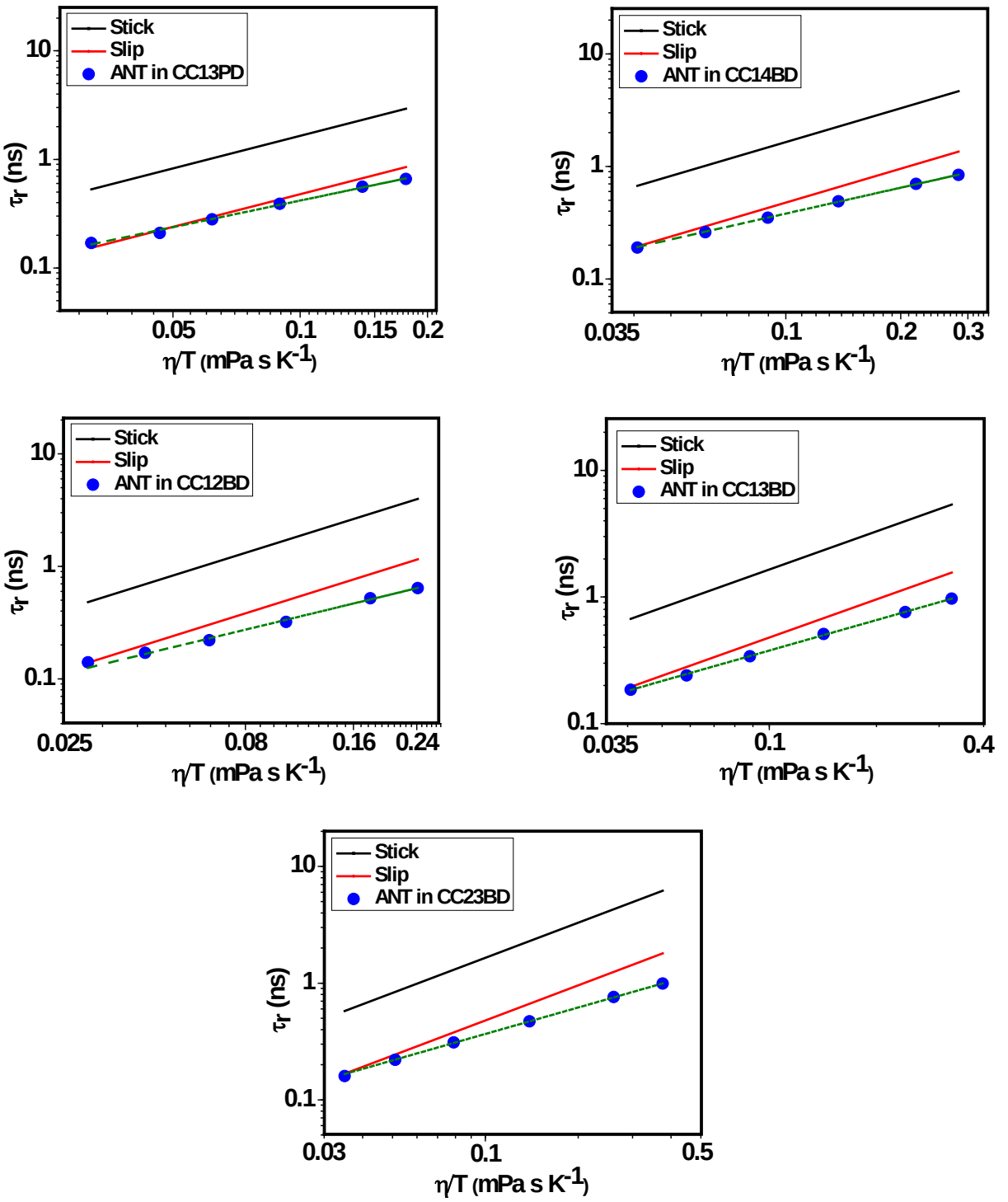


**Figure S6. Plots of $\tau_r$ vs η/T for ANT in DESs. The solid circles indicate the experimental rotational times and the dashed lines represent fit to the data according to $\tau_r = A(\eta/T)^p$. Computed stick (black) and slip (red) lines using SED theory are also shown.**

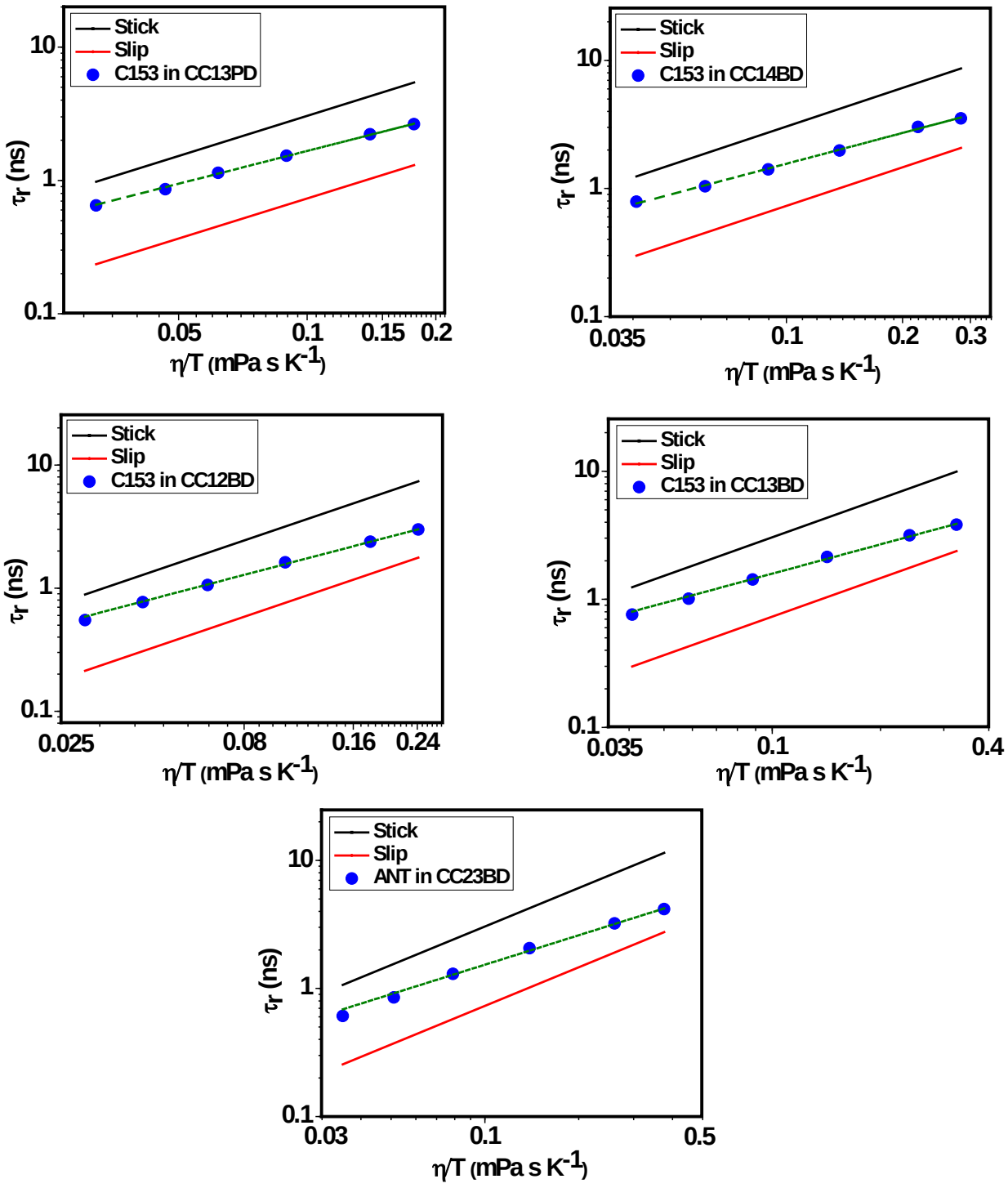


**Figure S7. Plots of $\tau_r$ vs η/T for C153 in DESs. The solid circles indicate the experimental rotational times and the dashed lines represent fit to the data according to $\tau_r = A(\eta/T)^p$. Computed stick (black) and slip (red) lines using SED theory are also shown.**

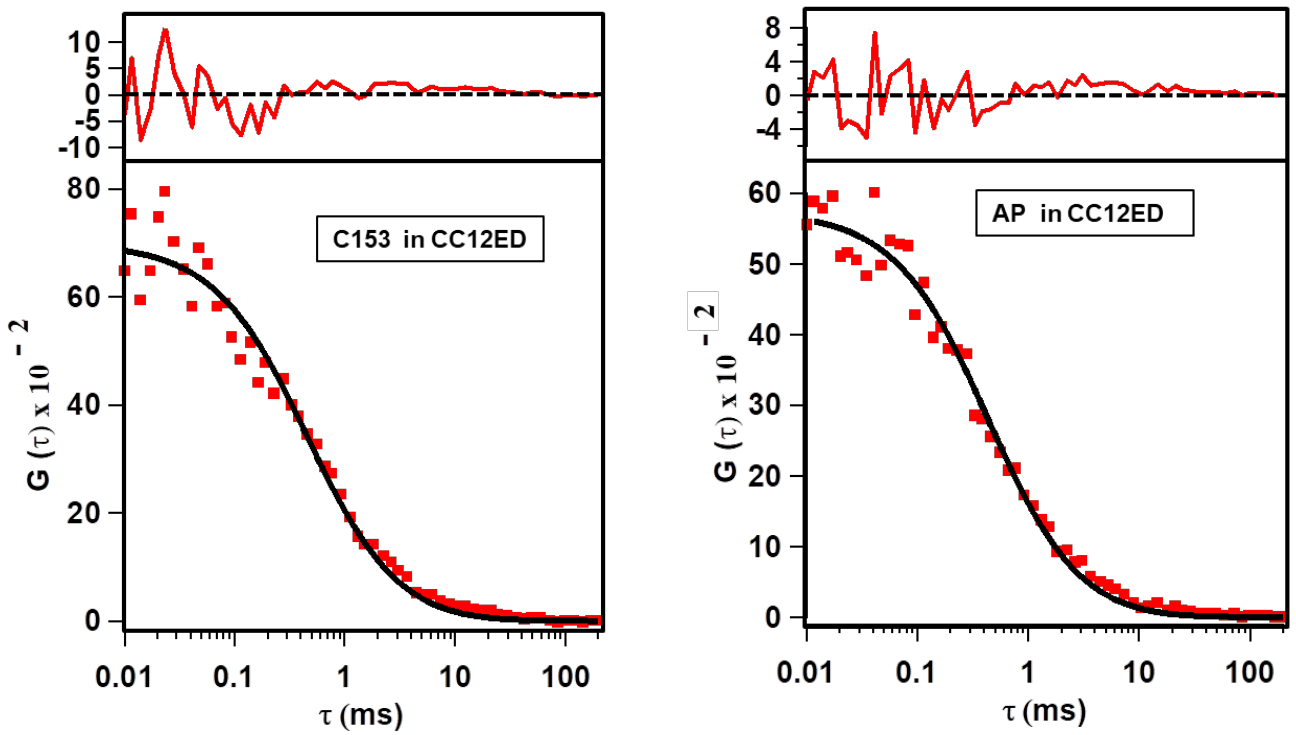


**Figure S8. Fluorescence correlation curves of the solutes in CC12ED system. The points are the experimental data, and the solid lines represent fit to the data using a single-component diffusion model. The residuals depicting quality of the fits are also shown at the top of each curve.**

**Table S1. Estimated Rotational Reorientation Times ($\tau_r$) of the Solutes in DESs at Different Temperatures.**

| DESs | Temp. (K) | Viscosity (cP) | Rotational reorientation time (ns) | | |
|---|---|---|---|---|---|
| | | | C153 | AP | ANT |
| CC12ED | 298 | 30.0 | 1.58 | 1.65 | 0.44 |
| | 303 | 24.5 | 1.30 | 1.37 | 0.36 |
| | 313 | 17.5 | 0.93 | 0.97 | 0.27 |
| | 323 | 13.5 | 0.69 | 0.71 | 0.19 |
| | 333 | 10.0 | 0.53 | 0.55 | 0.16 |
| | 343 | 08.0 | 0.43 | 0.44 | 0.13 |
| CC13PD | 298 | 53.0 | 2.64 | 3.14 | 0.66 |
| | 303 | 42.5 | 2.22 | 2.53 | 0.56 |
| | 313 | 28.0 | 1.53 | 1.83 | 0.39 |
| | 323 | 20.0 | 1.14 | 1.29 | 0.28 |
| | 333 | 15.5 | 0.86 | 0.96 | 0.21 |
| | 343 | 11.0 | 0.65 | 0.75 | 0.17 |
| CC14BD | 298 | 84.5 | 3.53 | 5.08 | 0.84 |
| | 303 | 66.5 | 3.02 | 4.00 | 0.70 |
| | 313 | 43.0 | 1.98 | 2.72 | 0.49 |
| | 323 | 29.0 | 1.41 | 1.87 | 0.35 |
| | 333 | 20.5 | 1.04 | 1.36 | 0.26 |
| | 343 | 14.0 | 0.79 | 1.00 | 0.19 |
| CC12BD | 298 | 72.0 | 2.99 | 5.30 | 0.64 |
| | 303 | 54.0 | 1.38 | 4.10 | 0.52 |
| | 313 | 32.5 | 1.62 | 2.50 | 0.32 |
| | 323 | 20.5 | 1.06 | 1.74 | 0.22 |
| | 333 | 14.0 | 0.77 | 1.18 | 0.17 |
| | 343 | 10.0 | 0.55 | 0.86 | 0.14 |
| CC13BD | 298 | 97.0 | 3.83 | 5.96 | 0.97 |
| | 303 | 73.0 | 3.16 | 4.75 | 0.76 |
| | 313 | 44.5 | 2.14 | 3.03 | 0.51 |
| | 323 | 28.5 | 1.43 | 2.02 | 0.34 |
| | 333 | 19.5 | 1.01 | 1.39 | 0.24 |
| | 343 | 14.0 | 0.76 | 1.05 | 0.18 |
| CC23BD | 298 | 112.0 | 4.17 | 7.20 | 0.99 |
| | 303 | 79.0 | 3.22 | 5.54 | 0.76 |
| | 313 | 43.5 | 2.06 | 3.09 | 0.47 |
| | 323 | 25.5 | 1.30 | 2.00 | 0.31 |
| | 333 | 17.0 | 0.85 | 1.33 | 0.22 |
| | 343 | 12.0 | 0.61 | 0.92 | 0.16 |